ISBN 978-83-927084-8-3
ISSN 0867-7964

EXPERIMENTAL STUDY OF BED FRICTION IN STRATIFIED FLOW WITH VISCOPLASTIC CARRIER IN PIPE

Václav Matoušek[1], Vojtěch Pěník[1], Lionel Pullum[2], Andrew Chryss[2]

1 Civil Engineering, Czech Technical University in Prague, Czech Republic, v.matousek@fsv.cvut.cz
2 CSIRO Mineral Resources Flagship, Bayview Avenue Clayton, Victoria, Australia. LionelPullum@CSIRO.au

The paper describes the observed behavior of a glass-bead bed driven to sliding by a Herschel-Bulkley liquid flowing in a 50-mm pipe. A transparent acrylic pipe in the horizontal section of our pipe rig enabled very clear visual observation of a stratified structure of the flow of the mixtures composed of transparent a Carbopol solution and transparent mono-size glass beads of the size 1.5 mm. The flow appeared to behave as a true two-layer system with the bed sliding 'en bloc' from the slip point at the deposition-limit velocity up to velocities at which a human eye could no longer follow particular grains in the bed. The flow was laminar above the stationary/sliding bed in the upper-plane bed regime. The fully-stratified structure of the slurry flow and its well defined conditions at low velocities provide an excellent opportunity to use the experimental data for a validation of components of a two-layer model. Based on the measured rheology of the carrier, measured integral parameters of slurry flow, and visually observed bed conditions the interfacial and wall friction of the bed could be evaluated. The paper discusses results of this analysis of the friction at the top of the bed and at the wall in contact with the sliding bed. It suggests appropriate friction formulae for the two-layer model to predict the viscous friction due to the flow of the non-Newtonian carrier as well as the mechanical friction due to transported particles at the boundaries of the stratified flow.

KEY WORDS: non-Newtonian, two layer model, laminar flow, tailings.

1. INTRODUCTION

Stratified flows with sliding beds can be modelled using a stratified layer model. Various versions of the model are available and typically they differ in the number of layers, formulae for boundary friction, and in case of partially stratified flow also in formulae for turbulent suspension support. In the literature, most models consider Newtonian carrier fluid, only few non-Newtonian carrier based models have been discussed. Pullum et al. (2004) presented a non-Newtonian version of a simple generic two-layer model for laminar and turbulent flow of power-law- and visco-plastic carriers. They used a broad experimental data set to show that model predictions were adequate at different flow conditions provided some model parameters had been established experimentally. Rojas and Saez (2012) introduced, and experimentally verified, their

version of a two-layer model to predict laminar and turbulent flows of non-Newtonian slurries of dense and fine (broadly graded) particles in a Casson fluid. For the laminar regime, they considered the flow above a stationary deposit only and used an assumption of equal shear stresses at the top of the deposit and the pipe wall discussed earlier by Pullum et al (2004).

Recently, we carried out laboratory experiments with pipe flows of a transparent mixture of non-Newtonian carrier and coarse grains. The flows were laminar and fully stratified with '*en bloc*' sliding bed behaviour and a developing shear layer at low velocities. At high velocities, the flows were turbulent and much less stratified, perhaps bed free. In this paper, we use one set of the experimental results for the laminar regime to evaluate friction of sliding bed driven by laminar flow of a visco-plastic carrier.

2. EXPERIMENT

2.1. MATERIALS

The tested slurry was composed of coarse glass beads (TK1.5; it was used as an analogue of coarse particles in thickened tailings handled in the mineral industry) and carrier fluids based on aqueous solutions of Carbopol polymer (Ultrez 10) (CBP; it was used as a model of non-Newtonian fluid with rheology typical for thickened tailings). The fraction of glass beads TK1.5 is virtually mono-disperse with d_{50} = 1.55 mm. Sieving tests showed that all grains were finer than 1.61 mm and coarser than 1.5 mm. Also, we tested the density of the beads (ρ_s = 2488 kgm^{-3}) and their concentration in loose poured bed ($c_{b,lp}$ = 0.61).

The CBP solution is a visco-plastic fluid of the Herschel-Bulkley (HB) type. Its density ρ_f = 1000 kgm^{-3} and rheological parameters vary with the mass concentration of CPB powder in water. In this paper, we discuss experiments with CBP fluid of the mass concentration 0.175 per cent. Samples of the CPB fluid were tested in the rotational viscometer (Haake VT550 with a standard sensor) before and after a pipe test. For the particular test discussed below, τ_y = 3.76 Pa, k = 2.034 Pa s^n, n = 0.48.

2.2. RIG

The tests were carried out in the experimental rig of the Water Engineering Laboratory of Czech Technical University in Prague (CTU). The rig is composed of horizontal and vertical pipes, a centrifugal pump and a sump tank, which can be bypassed during operation. The vertical U-tube serves to determine the mean delivered concentration of grains, C_{vd}, in flowing mixture. One part of a horizontal pipe contains a measuring section over which the differential pressure (expressed as hydraulic gradient, i_m, in meters of carrier over unit length of pipe), is measured. This horizontal part of the internal diameter D = 50 mm is made of transparent acrylic, the rest of the pipeline is made of PE (internal diameter 51.4 mm). The total length of the loop is 23 m, the measuring section is 1 m long. More details about the rig and measuring techniques can be found in Matoušek et al. (2013).

2.3. PARAMETERS MEASURED OR VISUALLY OBSERVED

The following sections refer to data points shown in Figure 1 which are tabulated here for convenience.

Table 1

Data Run values

Run	1	2	3	4	5	6	7	8	9
V_m (ms^{-1})	0	0	0.042	0.148	0.427	1.01	1.44	1.82	2.18
Run	10	11	12	13	14	15	16	17	18
V_m (ms^{-1})	2.50	2.81	3.10	3.41*	3.71	3.98	4.23	4.51	4.76

*laminar/turbulent transition velocity

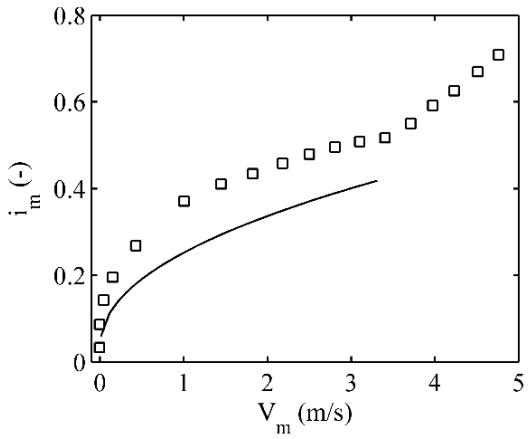

Figure 1 Flow resistance curve. Legend: squares – slurry flow measurement (runs Nos 1 to 18); line – carrier calculation for laminar flow.

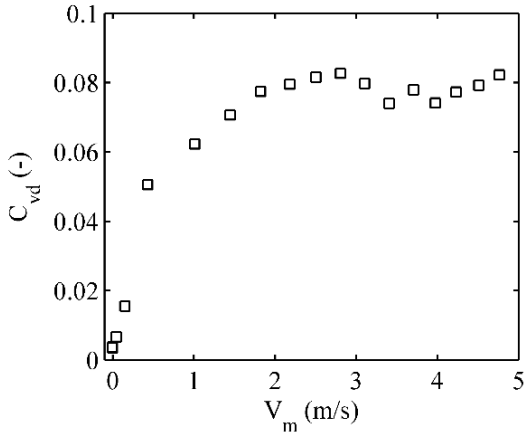

Figure 2 Development of mean delivered concentration with mean slurry velocity. Legend: squares – slurry flow measurement (runs Nos 1 to 18).

The test produced the measured curve for flow resistance (Figure 1) and the measured curve for delivered concentration of grains (Figure 2), both composed of 18 points representing 18 test runs detailed in Table 1. The shapes of the flow resistance curve and of the delivered-concentration curve demonstrate that there is no flow in the first two runs (runs Nos 1 and 2). The effect of the carrier fluid's yield stress is that the hydraulic gradient, i_m, must exceed 0.10 before flow occurs. Transition from laminar to turbulent flow occurs at $V_m \approx 3.4$ m/s (run No. 13). Also, Figure 1 shows that the presence of coarse particles considerably increases the hydraulic gradient (frictional pressure drop) in the laminar flow regime – compare the measured gradients for slurry with calculated gradients for carrier only at the same velocity in Figure 1.

The thickness of the sliding bed and the thickness of the shear layer were obtained from visual observations (Figure 3). At very low velocities in particular, the positions of the interfaces could be determined accurately. At Run No. 4, even the velocity of bed sliding, V_b, could be determined from the simple visual observations.

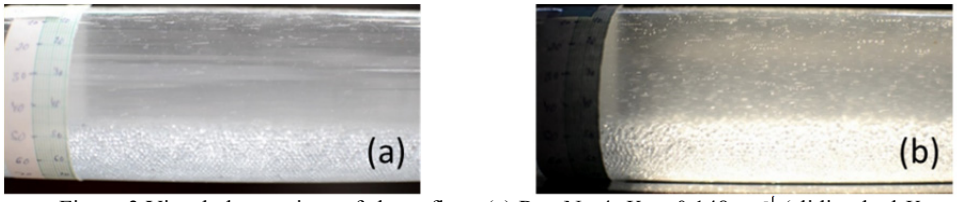

Figure 3 Visual observations of slurry flow, (a) Run No 4, $V_m = 0.148$ ms^{-1} (sliding bed, $V_b \approx 0.002$ ms^{-1}) , (b) Run No 5 $V_m = 0.427$ ms^{-1} (sliding bed)

2.4. VISUAL OBSERVATION OF THE FLOW

The flow appeared to be behave as a true two-layer system with the bed either stationary or sliding '*en bloc*' from the slip point at the deposition-limit velocity ($V_{dl} \approx 0.145$ m/s) up to velocities at which a human eye could no longer follow individual grains in the bed. Run No. 3 was a flow above the stationary deposit. The laminar flow (small bubbles in the flow served as tracers that confirmed that the flow was actually laminar) moved quite slowly over the bed and eroded just one layer of grains from the top of the bed. The Shields number ($\theta = \tau_i / [(\rho_s - \rho_f) g d_{50}] \approx 0.82$, where τ_i is the interfacial shear stress, g is the acceleration of gravity) at the interface was high enough to prevent a development of any bed forms, i.e. the erosion process took place in the upper plane bed regime.

Run No. 4 demonstrates stratification of flow just above the slip point (Figure 3a), the bed slides very slowly ($V_b \approx 2$ mm/s), the interface is sharp with a shear layer limited to just one grain layer. Run No. 5 shows stratified flow with faster sliding bed (Figure 3b). The flow remains laminar and stratified, the thickness of the shear layer tends to increase to approximately 2 grain layers. In order to recognize individual grains in the bed and the exact position of the interface, a bright LED light was used to illuminate the flow during run No. 5.

At higher velocities, still in the laminar regime, the thickness of the sliding bed decreases and the thickness of the shear layer increases with the increasing V_m.

3. ANALYSIS OF BED FRICTION

The fully-stratified structure of the observed slurry flow and its well defined conditions, i.e. laminar flow of the carrier, '*en bloc*' sliding of the bed, visually detectable thicknesses of the bed and of the shear layer and visually detectable velocity of sliding bed just above the slip point, provide an excellent opportunity to use these experimental results to evaluate a two-layer model with a non-Newtonian carrier. Based on the measured rheology of the carrier, the measured integral parameters of slurry flow (the average velocity, pressure drop, delivered concentration) and the visually observed bed conditions (the thickness of the sliding bed, y_b, thickness of the shear layer, H_{sh}), the interfacial and wall friction of the bed, and the coefficient of Coulombic sliding friction for the bed, μ_s,, can be evaluated.

For the bed analysis, the following questions are raised as subjects to investigate:

- How to use the laminar friction law for the top of the bed which slides and is subject to erosion (the shear layer is present)?
- How to assess viscous friction between the sliding bed and the pipe wall; how to calculate the viscous shear stress at the wall below the sliding bed?
- How to assess mechanical friction between the sliding bed and the pipe wall; how to calculate the force against the wall and what is a typical value of the coefficient of mechanical friction?

3.1. SHEAR STRESS AT TOP OF SLIDING BED

The shear stress at the top of sliding bed below the shear layer is composed of the carrier shear stress and the grain shear stress.

$$\tau_i = \tau_{fi} + \tau_{si} \qquad (1)$$

Carrier stress

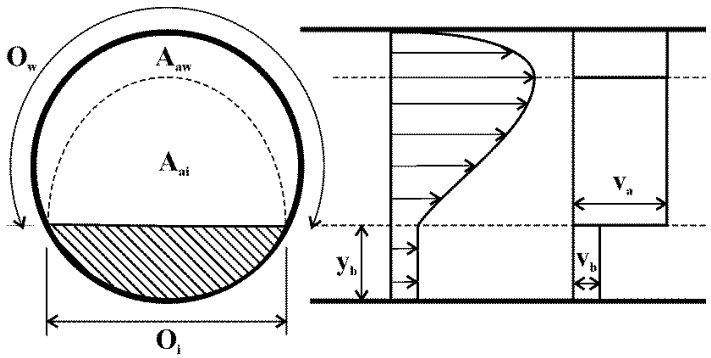

Figure 4 Schematic of sliding bed

For laminar flow above stationary deposit, the interfacial shear stress τ_{fi} may be considered equal to the shear stress at the pipe wall in the upper layer, τ_a (Pullum et al. 2004, Rojas and Saez 2012) since the shear stress is not a function of the surface roughness, unlike in turbulent flows. However, if the bed slides (the interface moves while the pipe wall remains stationary) and a shear layer develops, then it seems

appropriate to consider $\tau_{fi} \neq \tau_a$, with each stress being associated with a different hydraulic radius:

$$R_{hai} = A_{ai}/O_{i,} \text{ and}$$
$$R_{haw} = A_{aw}/O_a \quad (2)$$

where A_{ai}, A_{aw} are sub-areas of the cross-sectional area of the upper layer associated with the interface and the pipe wall, respectively; O_i, O_a are perimeters of the interface and the pipe wall, respectively (Figure 4).

The carrier component of the interfacial stress and wall shear stress takes the form

$$\tau_{fi} = f(V_i, R_{hai}, \tau_y, k, n), \text{ and}$$
$$\tau_a = f(V_a, R_{haw}, \tau_y, k, n) \quad (3)$$

where $V_i = V_a - V_b$ (V_a is the average velocity in the upper layer, V_b is the average velocity in the lower layer), is solved for the laminar flow of a HB-carrier using a momentum formula, e.g. the one proposed by Chilton and Stainsby (1998).

Grain stress

The shear stress exerted at the top of the sliding bed by colliding grains travelling in the shear layer is

$$\tau_{si} = \frac{1}{2}(\rho_s - \rho_f) g H_{sh} c_b tan\varphi' \quad (4)$$

in which $tan\varphi'$ is the coefficient of internal friction of colliding grains in the shear layer.

An iterative solution of the grain stress equation, momentum- and mass-balance equations for the upper layer leads to a determination of τ_a, τ_i, and V_b.

3.2. SHEAR STRESS BETWEEN SLIDING BED AND PIPE WALL

The total shear stress at the pipe wall below the sliding bed is the sum of the carrier stress (viscous friction) and the grain stress (mechanical friction),

$$\tau_b = \tau_{fb} + \tau_{sb} \quad (4)$$

Carrier stress

The carrier shear stress is a result of laminar shearing in between the pipe wall and the underside of the sliding bed. To determine the wall shear stress of the carrier, τ_{fb}, one option is to relate the stress with the hydraulic radius of the entire discharge area of the lower layer, $R_{hbw} = A_b/O_b$ (A_b is the cross sectional area of the lower layer, i.e. the bed, O_b is the perimeter of the pipe wall in contact with the bed), and then apply the momentum equation for laminar flow to obtain the shear stress as before.

An alternative approach is to assume that the region of carrier shearing above the pipe wall is confined to a thin layer between the wall and the sliding bed. For the laminar flow of the HB-carrier, a simple assumption is that the viscous shear stress at the pipe wall below the '*en bloc*' sliding bed is solved using the fluids constitutive equation with a strain rate given by V_b/d.

Thus the under-bed carrier stress can be determined by these two models

$$\tau_{fb} = f(V_b, R_{hbw}, \tau_y, k, n) \text{ or} \quad (5)$$

$$\tau_{fb} = \tau_y + k\left(\frac{V_b}{d}\right)^n$$

Grain stress

In the two-layer model, the shear stress exerted by sliding bed at the pipe wall is solved as a product of the coefficient of mechanical friction between sliding bed and pipe wall, μ_s, and the grain normal stress integrated over O_b. The grain stress is then

$$\tau_{sb} = \mu_s \frac{F}{O_b} \tag{6}$$

where either $F=F_w$ the submerged weight of the bed, or $F=F_n$ the hydrostatic normal force exerted by the bed against the wall.

A solution for the force balance in the bed using the chosen formulae for boundary stresses leads to a resulting value of the mechanical friction coefficient ($\mu_{s,Fn}$ or $\mu_{s,Fw}$).

3.3. MODEL COMPUTATIONS

The non-Newtonian two-layer model composed of force-balance and mass-balance equations and boundary friction formulae is solved for measured inputs (τ_y, k, n, ρ_f, ρ_s, d, D, V_m, i_m, C_{vd}), visually observed inputs (y_b/D, H_{sh}/D), and estimated values of model constants (c_b= 0.54 from visual observation of organization of grains in the sliding bed which indicates that the bed concentration may be close to simple cubic packing of spheres; $tan\varphi'$ = 0.32).

The model calculates the boundary stresses and gives values of V_b and μ_s as basic outputs. A value of V_b is a result of model balances in the upper layer, a value of μ_s is a result of the force balance in the lower layer. A solution of a set of the model equations in the upper layer requires iterations which must satisfy an equality of the computed value of the interfacial shear stress.

4. DISCUSSION

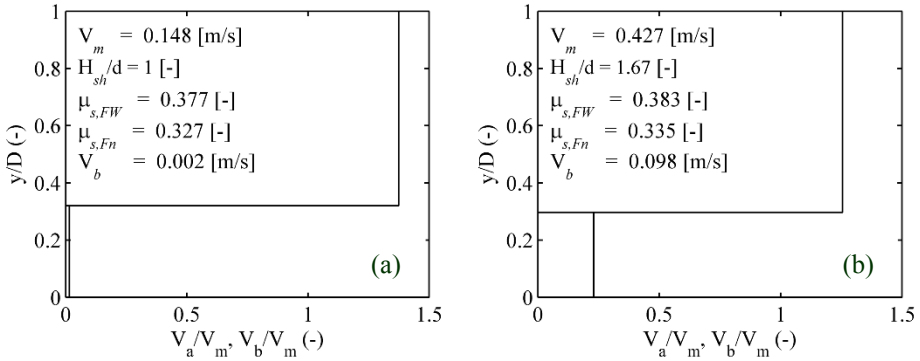

Figure 5 Computed two-layer velocity distribution for laminar flow for runs (a) No 4 and (b) No 5. Legend: values of model inputs (V_m, H_{sh}/d) and outputs ($\mu_{s,Fw}$, $\mu_{s,Fn}$, V_b)

Figure 5 shows model computation results for two different velocities (runs Nos 4 and 5) of the stratified laminar flow. For run No. 4 (Figure 5a) with inputs V_m = 0.148 m/s and H_{sh}/d = 1, the predicted value of V_b = 0.002 ms^{-1} which is in an excellent agreement with the visual observation and suggests that the proposed modelling of the interfacial shear stress is appropriate. The predicted values of $\mu_{s,Fn}$ and $\mu_{s,Fw}$ are also realistic suggesting that the modelling of the shear stress (here using the V_b/d-approach) at the pipe wall below the bed is appropriate too. However, runs with higher values of V_b need to be analyzed in order to evaluate suitability of the τ_{fb} modelling.

Run No. 5 (V_m = 0.427 m/s, Figure 5b) represents the situation where the bed slides considerably faster and the thickness of the sliding bed is slightly smaller. Also for this run, the prediction of the $\mu_{s,Fn}$ and $\mu_{s,Fw}$ values are realistic and thus supports a validity of the V_b/d-approach for the τ_{fb} modelling.

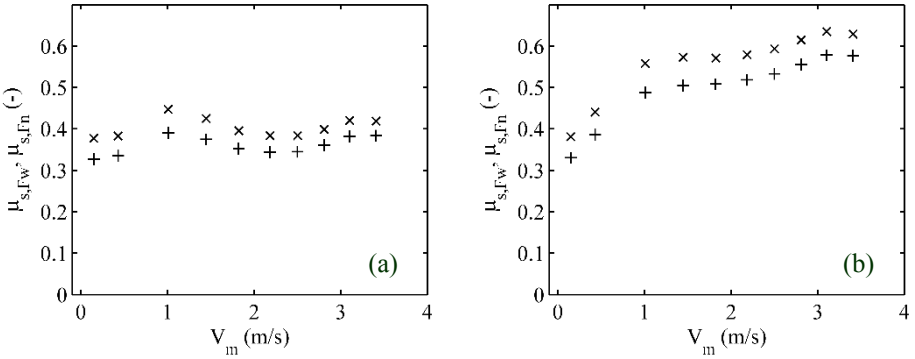

Figure 6 Coefficient of mechanical friction of sliding bed for runs Nos 4 to13 (laminar flow). (a) τ_{fb} modelled using V_b/d method; (b) τ_{fb} modelled using R_{hbw} method. Legend: x – $\mu_{s,Fw}$; + – $\mu_{s,Fn}$.

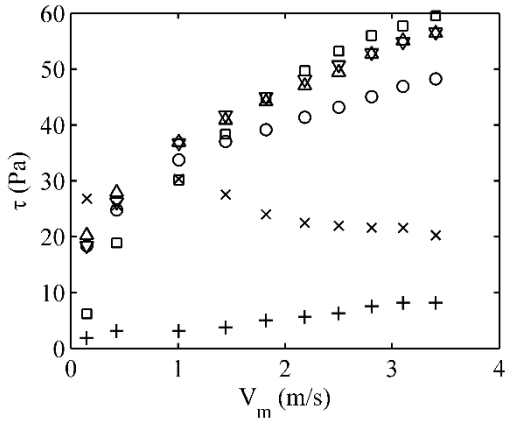

Figure 7 Boundary shear stresses in two-layer model for runs Nos 4 to 13 (laminar flow). Legend: ∇ – τ_a; Δ – τ_i; ○ – τ_{fi}; + – τ_{si}; x – $\tau_{sb,Fn}$; □ – τ_{fb} (τ_{fb} for V_b/d-method).

At higher velocities, the visual observation of y_b/D and H_{sh}/D is associated with more uncertainty. Nevertheless, observed values of the model inputs lead to very similar values of $\mu_{s,Fn}$ and $\mu_{s,Fw}$ as at low velocities (Figure 6a) indicating that the bed-friction modelling approach is appropriate. Use of the R_{hbw} method (Figure 6b) seems less appropriate as the resulting values of $\mu_{s,Fn}$ and $\mu_{s,Fw}$ increase with V_m which is unrealistic and indicates that the approach tends to underestimate τ_{fb}.

Figure 7 quantifies the calculated boundary shear stresses at different velocities in laminar flow (runs Nos 4 to 13). It shows that viscous stresses dominate over grain stresses at $V_m > 1$ m/s. Also, Figure 7 shows that boundary stresses at two different perimeters of the upper layer remain almost the same even though the bed slides and its top is eroded.

5. CONCLUSIONS

The results of the experimental study indicate that the friction formulae proposed for the non-Newtonian two-layer model are suitable for predicting the viscous friction due to the flow of the non-Newtonian carrier, as well as the grain friction, due to transported particles at the boundaries of the stratified flow. These results are typical of a series of experiments carried out at CTU and CSIRO.

The conclusions drawn from the analysis of the sliding bed in the visco-plastic carrier are as follows:

1. The laminar friction law is appropriate for the fluid shear stress at the erodible top of a sliding bed provided that the hydraulic radius is calculated for the sub-area associated with the interface. The grain stress from the developed shear layer contributes to the total interfacial shear stress and this contribution should not be neglected.
2. The viscous shear stress underneath the sliding bed contributes considerably to the total friction; it can be calculated using the rheological model expressed for the wall with the wall shear strain expressed as V_b/d.
3. A value of the coefficient of mechanical friction between the sliding bed (glass beads) and the acrylic pipe wall is of order 0.40 if it is related to the submerged weight of the bed in keeping with values quoted in the literature; the value is smaller if the normal force of the hydrostatic type is used to determine the bed load on the pipe wall, but it is believed that this method is inappropriate for large particles as reported here.

6. ACKNOWLEDGEMENTS

The authors would like to thank the following companies who have sponsored aspects of this work as part of the AMIRA P1087 project “Integrated tailings management”, i.e. Anglo American PLC, BASF Australia Ltd., Freeport-McMoRan Inc., Gold Fields Australasia Pty. Ltd., Outotec Pty. Ltd., Nalco-Ecolab Pty Ltd., Newmont Mining Corp., Shell Canada Energy Ltd. and Total E&P Canada Ltd.

REFERENCES

1. Chilton, R.A., Stainsby, R., 1998. Pressure loss equations for laminar and turbulent non-Newtonian pipe flow. J. Hyd. Eng. 124, 522-529.
2. Matoušek, V., Krupička, J., Picek, T., 2013. Validation of transport and friction formulae for upper plane bed by experiments in rectangular pipes. J. Hydrol. Hydromech. 61(2), 120-125.
3. Pullum, L., Graham, L., Slatter, P., 2004. A non-Newtonian two layer model and its application to high density hydrotransport. Proc. 16th Int. Conf. on Hydrotransport, Santiago de Chile.
4. Rojas, M.R., Saez, A.E., 2012. Two-layer model for horizontal pipe flow of Newtonian and non-Newtonian settling dense slurries. Ind. Eng. Chem. Res. 51, 7095-7103.